

LASER OBSERVATIONS OF WAVE GROWTH AND  
FOAM DENSITY FOR FETCH LIMITED 25 M/SEC WINDS

by

Duncan B. Ross  
National Oceanic and Atmospheric Administration  
Atlantic Oceanographic and Meteorological Laboratories  
Sea-Air Interaction Laboratory  
Miami, Florida

Vincent Cardone  
Department of Oceanography  
and Meteorology  
New York University

The variability of sea surface conditions has been observed from a low flying aircraft by a laser wave profiling system for fetch limited wind speeds of 25 M/SEC in the North Sea. Wave profiles obtained with the laser system have been analyzed and show that wave growth occurs simultaneously at all frequencies and that an equilibrium value for the higher frequency components is eventually reached, but not before substantially higher (overshoot) values are obtained. Simultaneous photography of the surface has been analyzed and show that 32% of the surface is covered with white caps, foam and streaks. This result is in good agreement with a semi-empirical relationship incorporating both the wind speed and the local wave spectrum which predicts 26% white water for the conditions observed.

## INTRODUCTION

For a number of years various scientific organizations have been concerned with developing techniques to remotely observe ocean surface parameters of wave height and wind speed in a quantitative manner. The purpose of these efforts is to provide information about the "state-of-the-sea" in support of operational requirements and to improve environmental forecasts.

During March of 1969, a study of the active and passive microwave characteristics of the ocean surface under the influence of various wind speeds and wave heights was staged out of Shannon, Ireland. This experiment was a cooperative effort of several scientific organizations and included three aircraft and scientists from the Naval Oceanographic Office, NASA Goddard Space Flight Center, NASA Manned Spacecraft Center, NASA AMES Research Center, New York University, and the University of Kansas. The three aircraft were equipped with a variety of remote sensors capable of measuring the microwave brightness temperature, radar backscattering cross section, surface temperature and wave heights.

Between March 6 and March 13, five coordinated flights were conducted over Atlantic weather stations "I" and "J" which are located within about 720 KM of Shannon and are routinely occupied by British and French weather ships. During these flights the highest winds encountered averaged about 16 m/sec, an unfortunate development as the sites were selected due to the high probability of occurrence of winds greater than 20 m/sec and seas greater than 8 meters. The weather situation was particularly interesting to the local Irish meteorologists who marveled at the "mildest weather in twenty years!"

As time was running out a weak meteorological disturbance formed just south of Ireland and moved slowly eastward while a building high pressure system moved eastward from Iceland into Norway between March 12 and March 14. As a result of these developments, the pressure gradient in the North Sea gradually increased and by 2300 GMT, March 13, offshore winds in the North Sea reached 20 m/sec.

By early morning, 14 March, it became apparent that these winds would hold, or increase, during the day and plans were made to conduct a flight experiment between the coast of Denmark and Scotland, the area of highest winds.

The plan of the experiment was to observe the behavior of the microwave signature of the surface under steady state wind conditions, but varying (growing) wave conditions. The NASA AMES Research Center Convair 990, a four engine jet aircraft, equipped with a scanning 19.35GHz microwave radiometer, a laser wave profiler, and a medium resolution infrared radiometer was utilized to obtain data from a distance of 160 kilometers off the coast of Denmark to the vicinity of the Shetland Islands. The NASA MSC P3A aircraft equipped with an active radar scatterometer was utilized to obtain radar cross section data at a point midway between the coasts of Denmark and Scotland. This report describes a portion of the results obtained with the laser wave profiler aboard the Convair 990.

## INSTRUMENTATION

### The Laser Wave Profiler

The laser wave profiler is a standard model Geodolite 3A airborne altimeter manufactured by Spectra Physics Inc., Mountain View, California (Figure 1). Figure (2) is a schematic diagram of the instrument.<sup>1</sup> The ranging technique consists of amplitude modulating a continuous wave helium-neon laser of red light centered at 6328 Å. The reflected light is collected by an 8 inch Schmidt Cassegrain telescope, detected by a photo multiplier, amplified and phase compared with the modulation frequency of the transmitted beam. The phase difference between these two signals is proportional to the transit time of the light, and hence the range. This range is directly proportional to the wave length of the modulation frequency. The highest modulation frequency available is 49.17MHz with a wave length of 3.048 meters. A total of five modulation frequencies are available yielding range selections of  $10^1$ ,  $10^2$ ,  $10^3$ ,  $10^4$  and  $10^5$  feet. By means of a range extender circuit each of these selections may be extended depending on the variability of the terrain. For wave measurements only the full scale increments of 3.048, 6.096 and 30.48 meters are used.\*

Static tests of the laser system have been conducted aboard an offshore tower.<sup>2</sup> Figures 3 and 4 are excerpted from reference (2) and show good agreement with a reference resistance wire wave staff.

Initial flight tests of the system were conducted off Atlantic City, New Jersey, and in the vicinity of ARGUS Island, a U. S. Navy Research Tower located near Bermuda, BWI, in 60 meters of water.

---

\* For more details the reader is referred to reference (1).

Figure 5 is an example of profiles of surface waves as they shoal and break on the beach shown in conjunction with simultaneous strip photography.<sup>3</sup> Figure 6 presents a comparison of averaged wave spectra obtained from three two-minute tracks flown near the ARGUS Island Tower with that derived from a twenty-minute sample of wave measurements obtained from the tower's resistance wire wave staff.

Since the aircraft is a moving reference, it is necessary to convert the observed wave spectrum to fixed coordinates. The conversion technique used involves accounting for the speed of the aircraft relative to the phase speed of each wave frequency component and assumes that all waves are traveling in the direction of the wind.<sup>4</sup> Since this is an approximation, the presence of swell and the spreading of wave energy with distance can lead to errors. In the case presented, little swell was present and the errors associated with directional spreading appear to be minimal for most purposes.

Another source of error is that of aircraft motions of heave, pitch, and roll. Figure 7 depicts the energy spectrum of heave motions, mapped to fixed coordinates, of the type of aircraft involved (a Lockheed Super Constellation) during the ARGUS Island experiment when the surface winds were 12 m/sec. It can be seen that essentially all of the aircraft heave (vertical) motions are concentrated at equivalent wave frequencies of less than .07HZ. The time series of roll angles experienced during this same three-minute track averaged about  $\pm 1.5^\circ$ . For flight altitudes of 200 M this corresponds to range (wave height) errors on the order of .15 meters. From these data, it can be seen that the majority of range errors associated with aircraft motions are small within the wave frequency pass band. As a result, the most convenient technique for removing these errors is simply high pass filtering, where the low frequency cut off selected depends upon the turbulence and, for most cases, is less than that associated with a true wave frequency of .07HZ. For extremely precise measurements, additional effort must be expended. For the data presented in this paper, the filtering technique was employed with apparently good results.

#### METEOROLOGICAL SITUATION

As noted in Section I, the general synoptic situation was a result of a weak disturbance moving eastward from Ireland simultaneous to an eastward displacement of a high pressure system located over Iceland. These two events caused a gradual tightening of the gradient in the North Sea and corresponding surface winds increased slowly, but steadily, to a maximum average of 25 m/sec by 1200 GMT, 14 March, as

reported by the German beacon vessel "LHHT", located at 57.7°N, 03°E (Figure 8).

Since only one of the reporting ships shown in Figure 8 was equipped with an anemometer (the rest being Beaufort estimates) it was felt necessary to derive the surface wind field by constructing isotachs of the geostrophic wind from a fine scale analysis of the surface pressure field.

Surface pressure data were obtained from a considerable number of British and continental shore sites and isotachs of the geostrophic wind were drawn relying heavily on the ship reports. Near the ship "LHHT", a ratio of surface (20m) to geostrophic winds of 70% gave good agreement although in nearby regions of large shear, higher geostrophic wind ratios are apparent. This is reasonable considering the effects of lateral turbulent momentum transfer. The above analysis considered the effects of stability after the technique of Cardone.<sup>6</sup>

In order to verify the validity of the inferred surface wind speeds, table 1 was constructed. This table shows wind speeds computed from the Litton model LTN 51 inertial system aboard the aircraft. The flight level winds reported are one minute averages computed approximately every five minutes during the lower altitude tracks. These values were averaged over twenty minutes of flight time (shown in brackets) and reduced to the equivalent twenty meter anemometer height assuming neutral stability and a logarithmic wind profile extending to an altitude of at least 43.3 meters.<sup>7</sup> The rather consistent agreement between the wind speeds derived by this technique, the geostrophic surface winds and the ship reports, lends considerable confidence to the presumed wind fields.

#### OBSERVATIONS OF WAVE GROWTH

The intent of the experiment was to begin the downwind flight track as near to the upwind shore as possible and then to fly downwind until the wave spectrum was essentially "fully developed". This was not entirely practical, however, as clearance procedural problems of the aircraft prevented approaching the shoreline within less than about 157 kilometers. Further, due to previous limited success because of relatively low wind speeds, the reported winds were greeted with some scepticism. As a result, the flight track (dashed line of Figure 8) was planned to best accommodate several possible meteorological situations which might be present, and events seem to confirm the final plan selected as a good compromise.

Figure 9 presents plots, at their appropriate fetches, of all available measurements of significant wave height,  $H_S^*$ . The fetch was measured as simply the distance from the coastline in the direction of the implied surface wind direction. It is seen that  $H_S$  generally increased with fetch to about 370KM but decreased thereafter. As a reference, a theoretical relation (Inoue-Cardone) is plotted for 22 m/sec, a suitable wind speed for much of the data as determined from the analysis of all available wind inputs.<sup>6</sup> The wind speed for the particular location of each  $H_S$  plotted was obtained from the geostrophic analysis and is shown below each value. Up to 370 kilometers the variation of  $H_S$  with fetch is in good agreement with the theoretical relation, which applies for infinite duration, fetch limited seas. Beyond 370 KM, the measured wave heights are considerably below the theoretical relation and depart increasingly with fetch. This latter behavior is generally explainable by duration effects, as the latter measurements plotted are from a wind field that exhibited considerable variability in wind duration. In particular, the durations are considerably longer in the near shore (southernmost portion of the first downwind run) area. An inspection of the previous six-hourly sea level pressure analysis indicate no significant variation in the pressure gradient there for the 24 hours preceding the flight. Considering that the winds prior to 24 hours were only slightly lower, these durations are probably sufficient for the seas to be fully developed at their respective fetches. From the vicinity of "LHHT" northwestward, however, the durations are extremely limited. The 3 hourly wind reports at "LHHT", Figure 10, suggest that the duration of 20 m/sec winds was only about 12 hours and that duration of 23 m/sec winds (or higher) was only about 3 hours. Toward the end of the last downwind run, durations were probably more limited, considering the way in which the synoptic scale pressure gradient was changing.

The behavior of the data below 370 KM suggests that these data might be employed to study growth, as the wind field there might be considered to be reasonably steady and homogeneous.

### Results

A convenient way to study the gross behavior of a developing sea in this case is presented in Figure 11 which shows the plots of spectral density ( $M^2$ -sec) as a function of frequency (true) and fetch. This contour analysis is based upon spectra computed for 160 KM, 176 KM, 203 KM, 231 KM, 268 KM, and 323 KM fetches. Though this resolution

---

\*  $H_S$  is defined as the average value of the highest one third waves.

is not as great, the analysis is conveniently comparable to those obtained in the radar altimeter fetch-limited study at lighter winds by Barnett and Wilkerson.<sup>8</sup> The analysis in Figure 11 is considerably smoother than those of their study, largely due to the decreased resolution. The major features to be deduced from this figure are:

1. At frequencies above about .13 Hz, the spectral density does not change significantly with fetch. Thus these spectral components are already saturated, or fully developed, and in equilibrium with the wind field.
2. Below about .13 HZ, all spectral components are increasing in intensity with fetch simultaneously.
3. The spectral peak generally moves toward lower frequencies (as indicated by dashed line) with increasing fetch, in general agreement with existing concepts of spectral development. A rather surprising feature, however, is that the magnitude of the spectral density at the peak does not increase markedly with fetch beyond about 185 KM.
4. A given spectral component will overshoot its eventual equilibrium value. That is, if the development of a single frequency component is followed fetchwise, it is seen that the spectral density increases rapidly to a maximum value at a given fetch and then decreases gradually to a lower equilibrium value at greater fetch. The effect is most noticeably between frequencies of .095 and .115. The overshoot effect at higher frequencies is not observed but presumably occurred at shorter fetches (160 KM) as the data suggest that the fetch at which the effect occurs increases with decreasing frequency. This striking feature of the North Sea spectra is perhaps the most remarkable, as it implies the operation of mechanisms in wave generation not yet treated satisfactorily by existing theories. The "overshoot" effect has been reported in wave tank studies and in the field experiment of Barnett and Wilkerson and its appearance here lends support to the fact that this is a "real" phenomena.<sup>9,10</sup> The magnitude of the overshoot effect observed in the Barnett and Wilkerson study, that is, the ratio of spectral density at eventual equilibrium to that at the peak of the overshoot, was scattered between .35 and .75. For the North Sea mission, this ratio could only be computed for frequencies of .111Hz, .108Hz, and .105Hz where values of .38, .50, and .41 occurred.

Some of the features discussed above are evident if the spectral density is plotted versus fetch for selected frequencies. Thus Figure 12a shows a saturated frequency. Superimposed upon the data

is the spectral behavior for the Inoue-Cardone growth theory which is based upon a modified Miles-Phillips resonance instability growth mechanism and the Pierson-Moskowitz fully developed spectrum.<sup>6</sup> It is seen that generally in 12 a-f, the equilibrium value observed is 30-40% less than that indicated by theory. This is largely explainable by the different equilibrium range constant of  $.52 \times 10^{-2}$  found for the North Sea spectra as compared to  $.8 \times 10^{-2}$  used in the Pierson-Moskowitz spectra. The overshoot effect is clearly evident in Figure 12 b-h. The theoretical growth, of course, does not indicate overshoot, as it is based upon the relation (in the early stages of growth)

$$\frac{d(S)}{dt} = A+BS \quad (1)$$

where S is spectral density, t is time, A is the resonance mechanism parameterization and B is the instability mechanism parameterization. Dissipation effects are included by allowing the growth rate to decrease as the fully developed spectral value is approached. For infinite duration limited fetch growth, (1) is written:

$$C_g \frac{ds(f)}{dx} = A+BS(f)$$

where X is the fetch, and  $C_g$  is the group velocity of each wave frequency, f. Disregarding the effect of the overshoot, it may be said that the Inoue-Cardone growth (which predicts the variation of  $H_S$  fairly well) is too fast for frequencies above .078Hz and too slow for frequencies below .069Hz. The rapid growth of these frequencies is surprising, especially considering that these spectral components should be under the influence of dissipation by bottom friction.

It is possible to quantitatively compute the values of A and B from plots 12, a-o, provided dissipation effects can be considered to be small (not considering bottom friction) if the spectral density is less than 30% of its eventual equilibrium value\*. Within this restriction, the computation can be performed on frequencies .087, .083, .078, .074, .069, and .063 Hz and will be performed on spectra recomputed for greater fetchwise resolution.

---

\* After Barnett and Wilkerson

WHITE CAP COVERAGE

A semi-empirical theory for the dependence of foam cover on wind speed and sea conditions has been proposed by Cardone.<sup>6</sup> An important part of the theory is the model used to describe the growth of the wave spectrum due to energy transferred from a turbulent wind profile - this model is also used in the wave forecasting schemes developed at New York University.

The growth rate of a spectral wave component  $S(f)$  in terms of the wind field specified at 19.5 meters above the sea surface, and the friction velocity  $U_*$  defined as  $\sqrt{\frac{\tau}{\rho}}$ , where  $\tau$  is the surface stress and  $\rho$  is the air density, may be described as

$$\frac{dS(f)}{dt} = A(f, U_{19.5}) + B(f, U_*) \cdot S(f) \left( 1 - \frac{S(f)^2}{S_{\infty}} \right) \quad (2)$$

where  $S(f)$  = spectral intensity at frequency

A = Phillips Resonance growth term

B = Miles-Phillips Instability Growth term

$S_{\infty}$  = Pierson Moskowitz Fully Developed Spectrum

The value of the term  $U_*$  depends upon the local wind field and the air-sea temperature difference. All non-linear dissipative mechanisms that would act to limit growth are modeled implicitly by the use of the term

$$1 - \left( \frac{S(f)}{S_{\infty}} \right)^2$$

which causes each spectral value to approach its equilibrium or saturated value given by the Pierson-Moskowitz formula.  $S(f)$  which is a function of wind speed and frequency and does not take into effect the overshoot phenomena discussed earlier.

The Phillips resonance term can be thought of as an initial excitation mechanism - necessary to start growth for parts of the spectrum with no energy initially - but small in comparison to the instability growth term which is responsible for nearly all the energy transfer.

Energy transfer does not cease after a spectral component reaches its equilibrium value, and the energy thus transferred can be thought of as being dissipated in wave breaking. Whitecaps are a manifestation of wave breaking and thus the whitecap coverage may be closely related

to the energy transfer to the fully developed portion of the spectrum. This energy transfer is given by the expression:

$$E = \rho_w \cdot g \cdot \int_0^{\infty} B \cdot S \cdot \delta \cdot df \quad (3)$$

where  $\delta = 1$  when  $S = S_{\infty}$   
 $\delta = 0$  when  $S < S_{\infty}$

This hypothesis was tested with the whitecap data obtained photographically by Monahan<sup>11</sup> on the Great Lakes. The spectral growth model was used to hindcast the wave spectrum for each case reported by Monahan from corresponding estimates of stability, wind speed, and fetch (durations were unknown and assumed to be infinite). The energy transferred to the fully developed portion of the spectrum was then correlated with the observed whitecap percentage. The resulting linear regression is shown in equation 4.

$$W_F = - .0185 + .893 \times 10^{-3} \cdot E(\text{ergs/cm}^2/\text{sec}) \quad (4)$$

where  $W_F$  = Fresh Water foam density in percent  
 $E$  = Energy dissipated in breaking waves.

Salt water whitecaps are apparently more persistent than fresh water whitecaps due to differences in the bubble-size spectra and hence for similar conditions of wave breaking, whitecap coverage should be expected to be greater over the oceans. An approximate salt water correction factor of 1.5 has been suggested by Monahan from results of a laboratory study of comparisons of fresh water and salt water whitecap data.<sup>12</sup>

An example of the computation of percent whitecaps is shown in Figure 13 for a wind speed of 25 m/sec and fetch of 180 n.mi. The dashed line is the fully developed spectrum for 25 m/sec, the solid curve is the hindcasted spectrum for a fetch of 180 n.mi. and the dash-dot line shows the contribution of the factor  $B \cdot S$  to the energy dissipation computation. The significant wave height is calculated to be 26 feet. The salt water whitecap cover is computed to be 26%. This result compares favorably with the value of 32% calculated from photography obtained during the North Sea experiment.

Figure 14 is an example of white cap conditions for the 25 m/sec winds observed during this flight. Note the large amount of surface area covered by thin streaks oriented in the direction of the wind. Figure 15 is an example of white-cap density for a 12 m/sec wind speed. The most striking difference between the two is in the amount of streaking evident. This characteristic of the wind driven ocean is important when considering the relationship of remotely obtained micro-wave signatures of the ocean to the surface wind and wave conditions.

### CONCLUSIONS

By the use of Photographic and Laser observations of sea surface conditions it has been found:

1. Existing wave theory can be used with good results to predict the rate of growth of the significant wave height with increasing fetch.
2. A migration of the spectral peak toward lower frequencies with increasing fetch is observed.
3. All wave frequencies are receiving energy simultaneously.
4. The spectral density of a particular frequency component will overshoot its eventual equilibrium value by as much as 50%.
5. Semi-empirical calculations of white cap density based on the rate of energy transfer and the state of development of the wave spectrum agree well with observations for the nearly fully developed case.

It should be noted that wave and white cap data such as discussed herein are very difficult to obtain. Thus extension of these results to other conditions of wind speed, fetch, and stability must be done with caution. Experimental efforts are continuing in this area and the emphasis will be on the short fetch and stability criterion and the characteristics of the surface driven by extremely high winds such as associated with hurricanes. These studies will be conducted both in a laboratory wave tank and in the field and should contribute significantly to future theories describing the wind driven seaway.

### ACKNOWLEDGEMENTS

The authors are grateful to the many persons who contributed toward this experiment and particularly the scientific and flight crew of the CV990 who responded to extremely short notice and made the North Sea flight possible. Special gratitude is extended Mr. J. W. Sherman, Dr. W. J. Pierson, and Dr. W. Nordberg for their aid and encouragement during all aspects of this effort, and particularly to the Irish Meteorologists at Shannon International Airport whose interest, assistance, and spirit contributed significantly to a successful and memorable experiment.

## References

- (1) H. Jensen and K. A. Ruddock, "Applications of a Laser Profiler to Photogrammetric Problems", presented at the American Society of Photogrammetry, Washington, D. C. 1965.
- (2) D. B. Ross, R. A. Peloquin and R. J. Sheil, "Observing Ocean Surface Waves with a Helium Neon Laser", Proceedings of the 5th Symposium on Military Oceanography, Panama City, Florida, May 1968.
- (3) V. E. Noble, R. D. Ketchum and D. B. Ross, "Some Aspects of Remote Sensing as Applied to Oceanography", Proceedings of the IEEE, Vol. 57, No. 4, April 1969.
- (4) M. St. Denis and W. J. Pierson, "On the Motions of Ships in Confused Seas", Trans. Soc. Nav. Arch. and Mar. Eng., 1961.
- (5) C. Catoe, W. Nordberg, P. Thaddeus and G. Ling, "Preliminary Results from Aircraft Flight Tests of an Electrically Scanning Microwave Radiometer", Goddard Space Flight Center Tech. Report No. X-622-67-352, August 1967.
- (6) V. J. Cardone, "Specification of the Wind Field Distribution in the Marine Boundary Layer for Wave Forecasting", Geophysical Science Laboratory, New York University, Report No. TR69-1, December 1969.
- (7) L. Moskowitz, "Reduction of Ocean Wind Data by use of Drag Coefficients with Application to Various Wave Forecasting Techniques", U. S. Naval Oceanographic Office, IMR No. 0-66-64, January 1965.
- (8) T. P. Barnett and J. C. Wilkerson, "On the Generation of Ocean Wind Waves as Inferred from Airborne Radar Measurements of Fetch-limited Spectra," Journal of Marine Research, Vol. 25, Number 3, September 15, 1967, pp 292-328.
- (9) A. J. Sutherland, "Growth of Spectral Components in a Wind-Generated Wave Train", J. Fluid Mech, Vol. 33, 1968.
- (10) H. Mitsuyasu, "On the Growth of the Spectrum of Wind-Generated Waves (II)," Reports, Res. Inst. Appl. Mech., Kyushu University, Vol. XVII, No. 59, 1969.
- (11) Monahan, E. C., "Freshwater Whitecaps", J. Atmos. Sci., Vol. 26, No. 5, 1969.
- (12) Monahan, E. C., "Laboratory Comparisons of Freshwater and Salt Water Whitecaps, J. Geophys. Res., Vol. 74, No. 28, 1969.

TABLE I  
 A COMPARISON OF WINDS OBTAINED FROM THE NASA CV990 OVER THE NORTH SEA AND 20-METER LEVEL WINDS  
 REDUCED FROM GEOSTROPHIC WINDS BASED UPON THE ANALYSIS SHOWN IN FIG. 3

Time (GMT)	Latitude	Longitude	Altitude (meters)	Flight Level		Reduced Geostrophic	
				Wind Direction	Wind Speed (m/s)	Wind Direction	Wind Speed (m/s)
1338	54°40'N	06°02'E	152	085°	23.7	110°	22.7
1345	55°15'N	06°01'E	152	112°	25.8 [25]	110°	22.7
1350	55°34'N	06°01'E	146	110°	23.1	110°	22.7
1355	55°56'N	06°03'E	116	110°	26.8	110°	22.7
1400	56°07'N	05°24'E	122	110°	22.7	110°	22.7
1407	56°13'N	04°30'E	152	098°	26.8	110°	23.7
1414	56°25'N	03°33'E	152	105°	27.3 [27.3]	110°	24.7
1417	56°28'N	03°12'E	152	107°	22.7	110°	25.8
1420	56°39'N	02°57'E	146	105°	29.9	110°	26.8
1435	57°35'N	02°17'E	152	107°	28.3	110°	25.8
1440	58°02'N	01°32'E	152	105°	25.8 [27.8]	110°	25.2
1445	58°14'N	01°10'E	152	110°	27.3	110°	25.2
1450	58°30'N	00°36'E	152	110°	30.4	110°	24.7
1455	58°48'N	00°01'E	152	108°	25.8	110°	23.7
1500	59°04'N	00°31'W	152	107°	24.7 [24.2]	110°	23.2
1505	59°23'N	01°06'W	152	108°	25.8	110°	22.7
1510	59°46'N	01°27'W	152	112°	21.6	110°	21.6

Note: Flight-level winds averaged over approximately 20-minute legs shown in brackets. The second value italicized is the aircraft value reduced to the 20-meter level after Moskowitz [7].

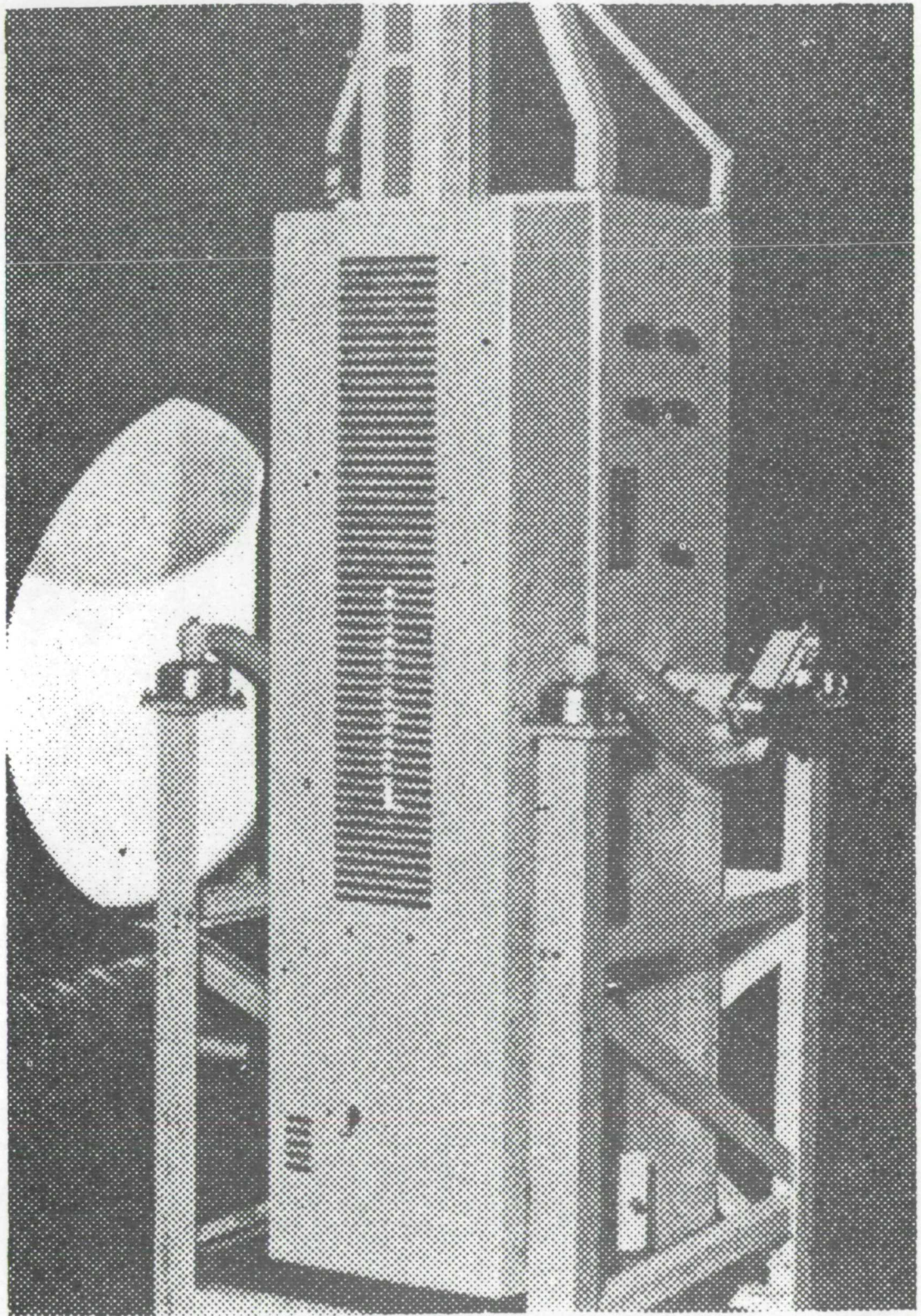


Fig. 1. Geodolite 3A laser profilometer.

# GEODOLITE BLOCK DIAGRAM

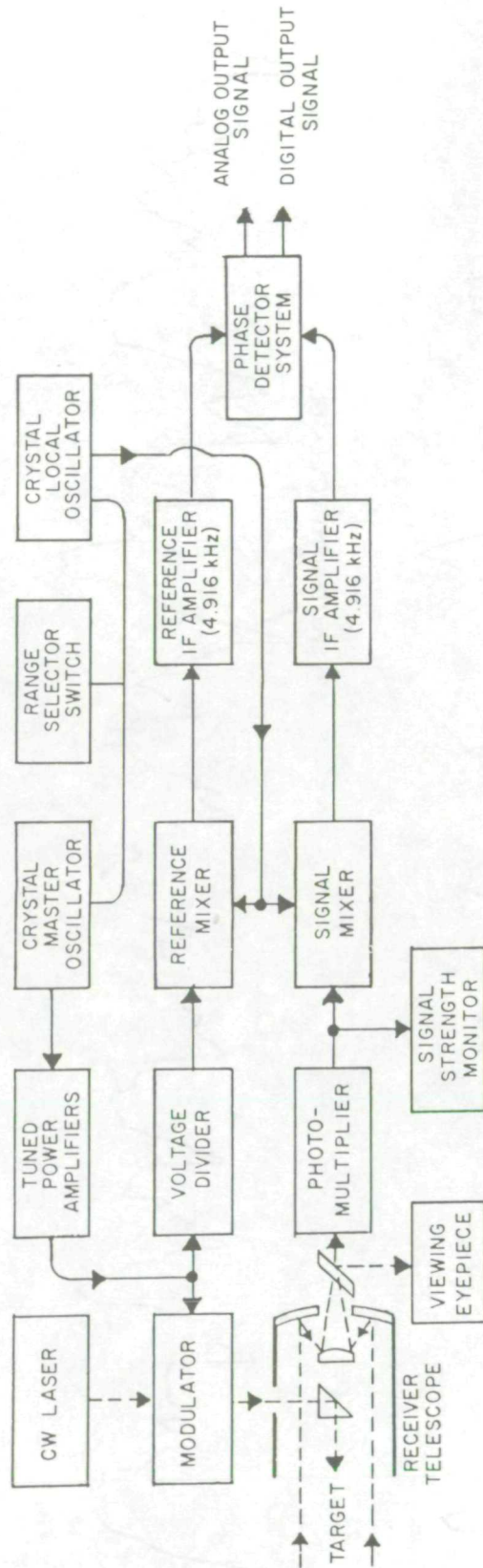


Fig. 2

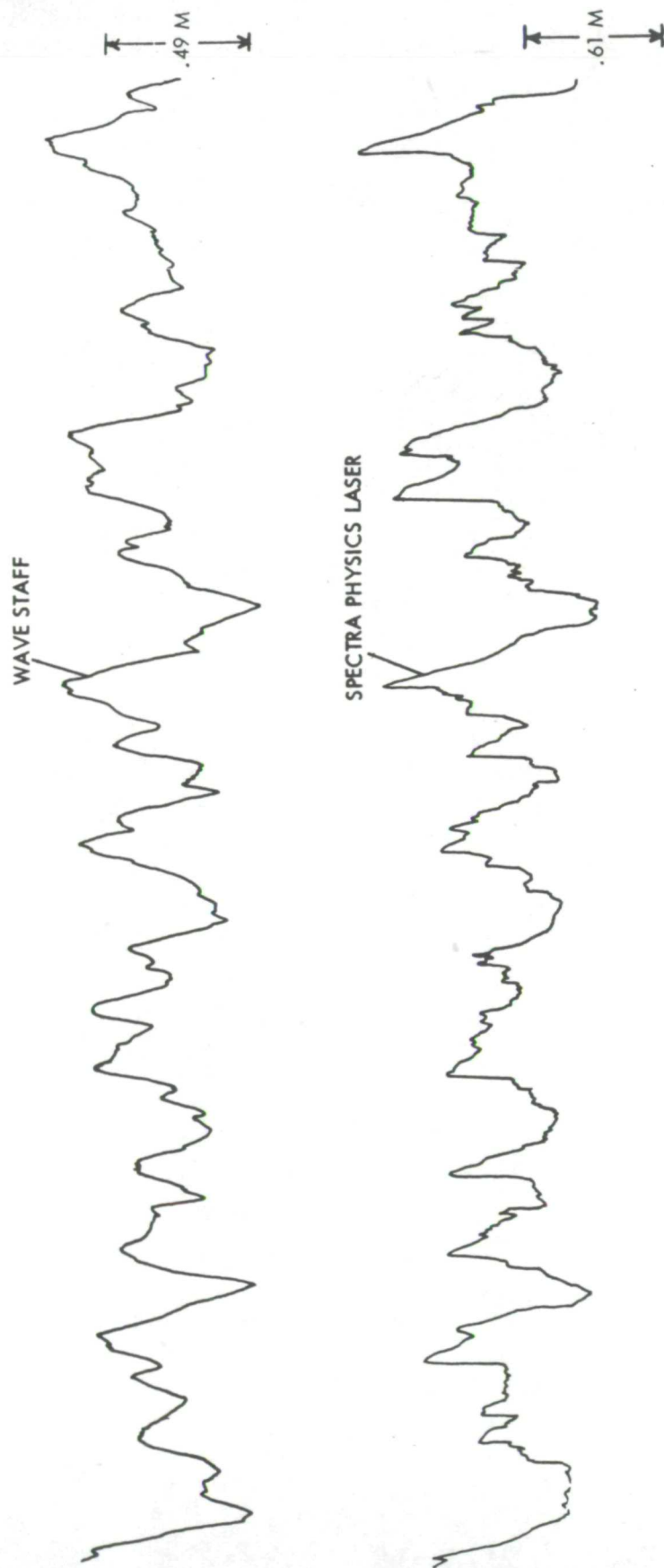


Fig. 3. Comparison of laser and wave-staff recordings of surface waves from a fixed ocean platform.

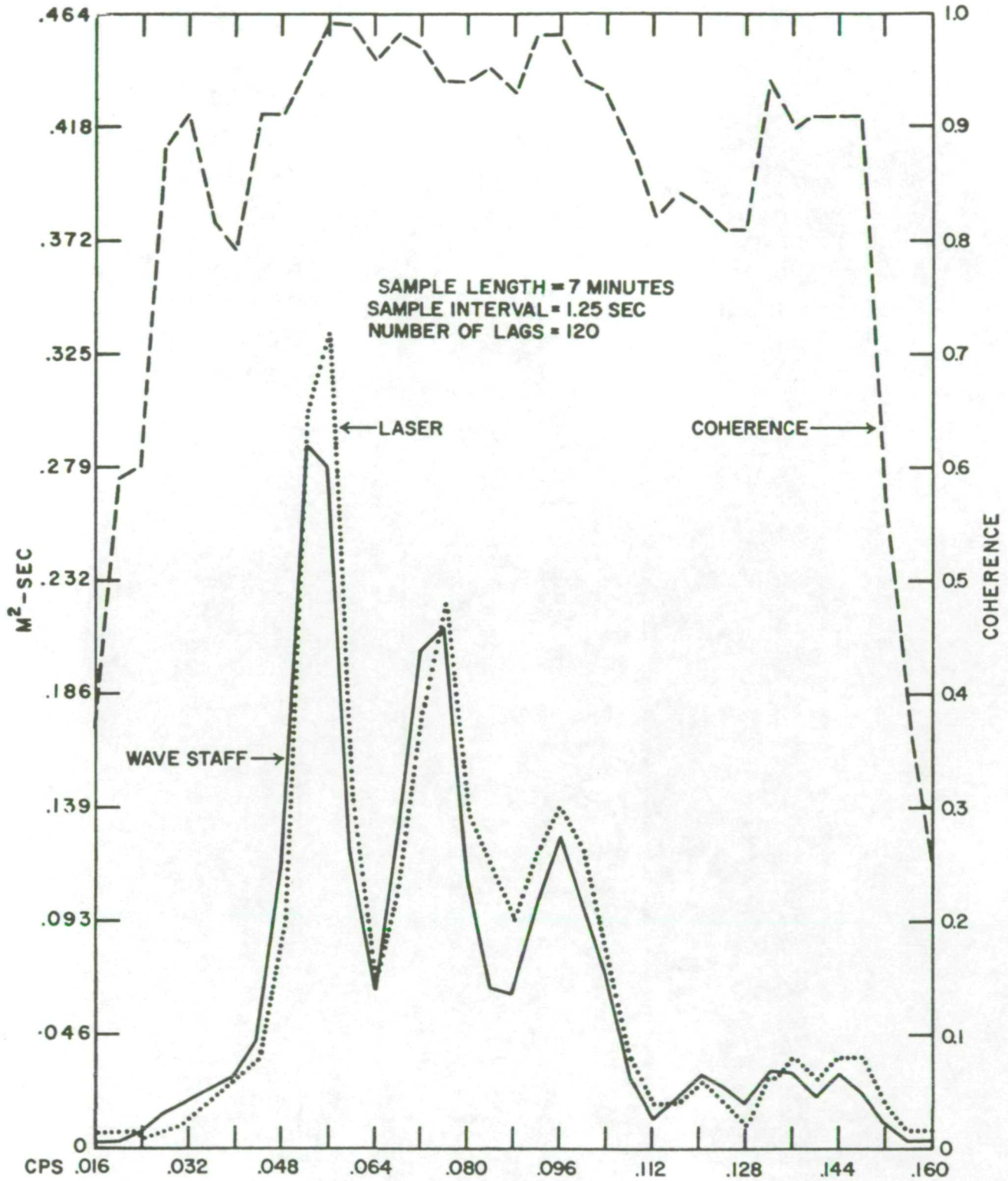


Fig. 4. Comparison of wave-energy spectra derived from laser and wave-staff recordings of surface waves.

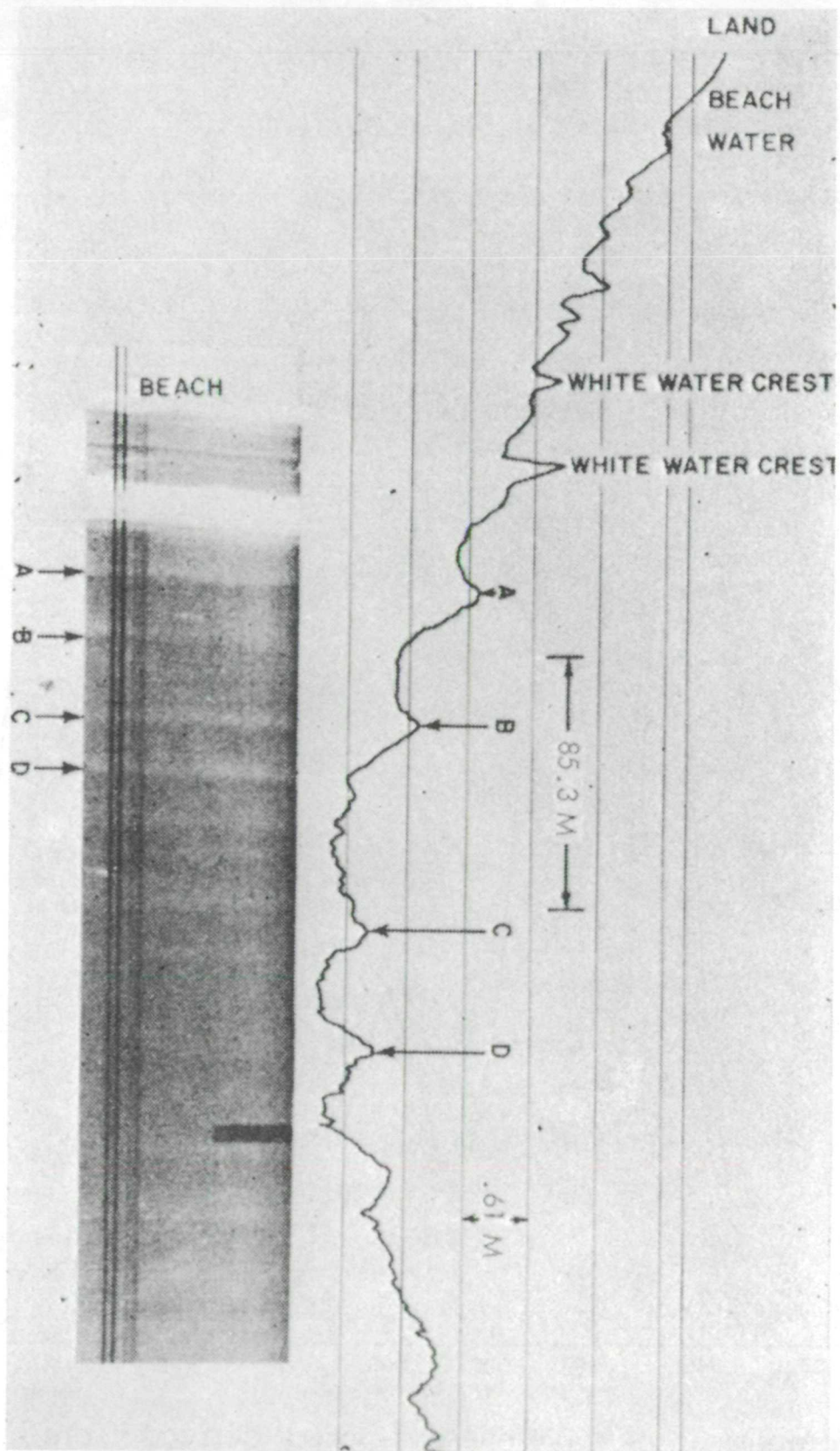


Fig. 5. Airborne laser profiles of surface waves obtained in conjunction with simultaneous continuous strip photography.

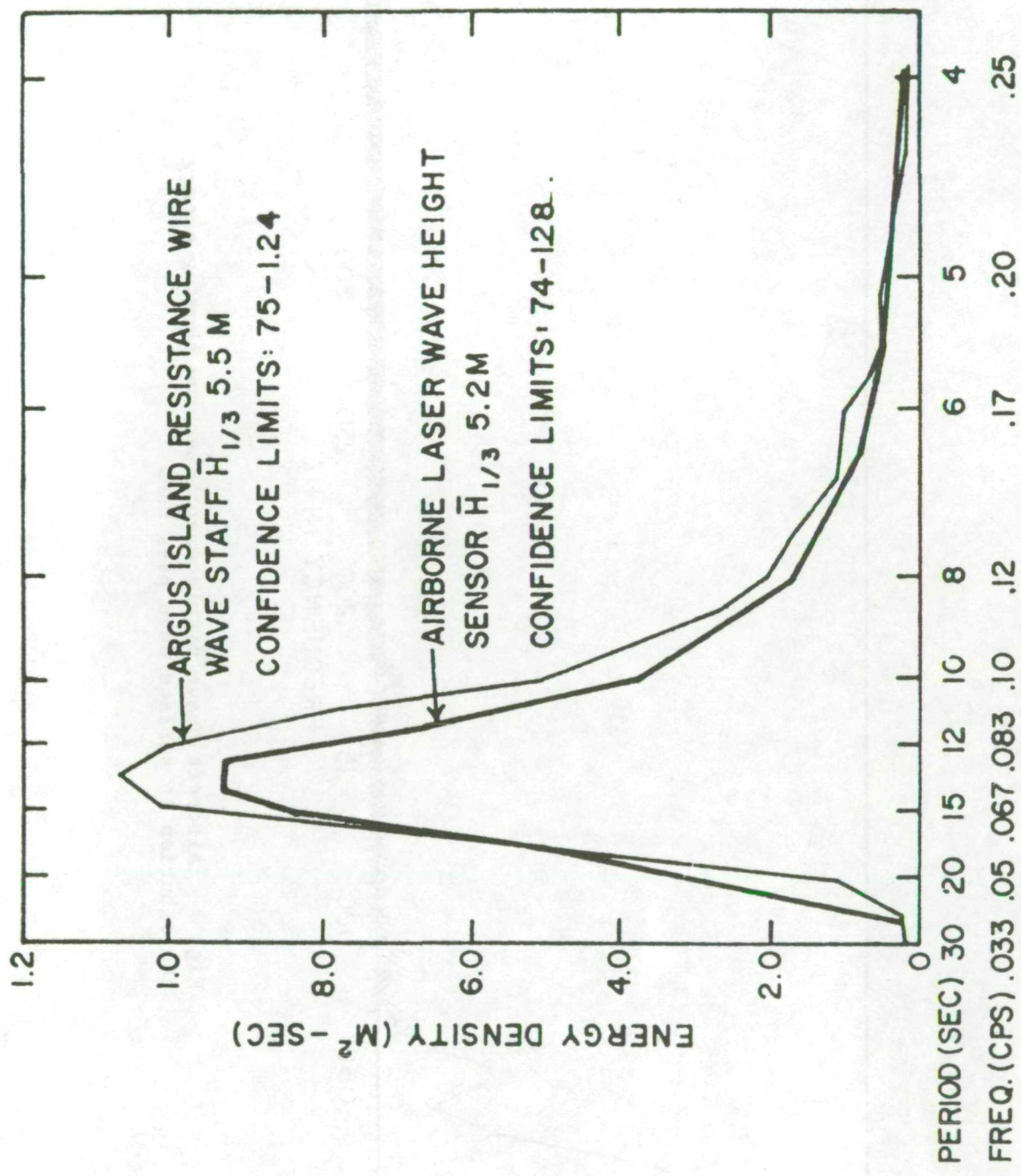


Fig. 6. Comparison of wave-power spectra obtained with the laser profiles aboard a U. S. Navy aircraft with that obtained from an *in-situ* wave staff.

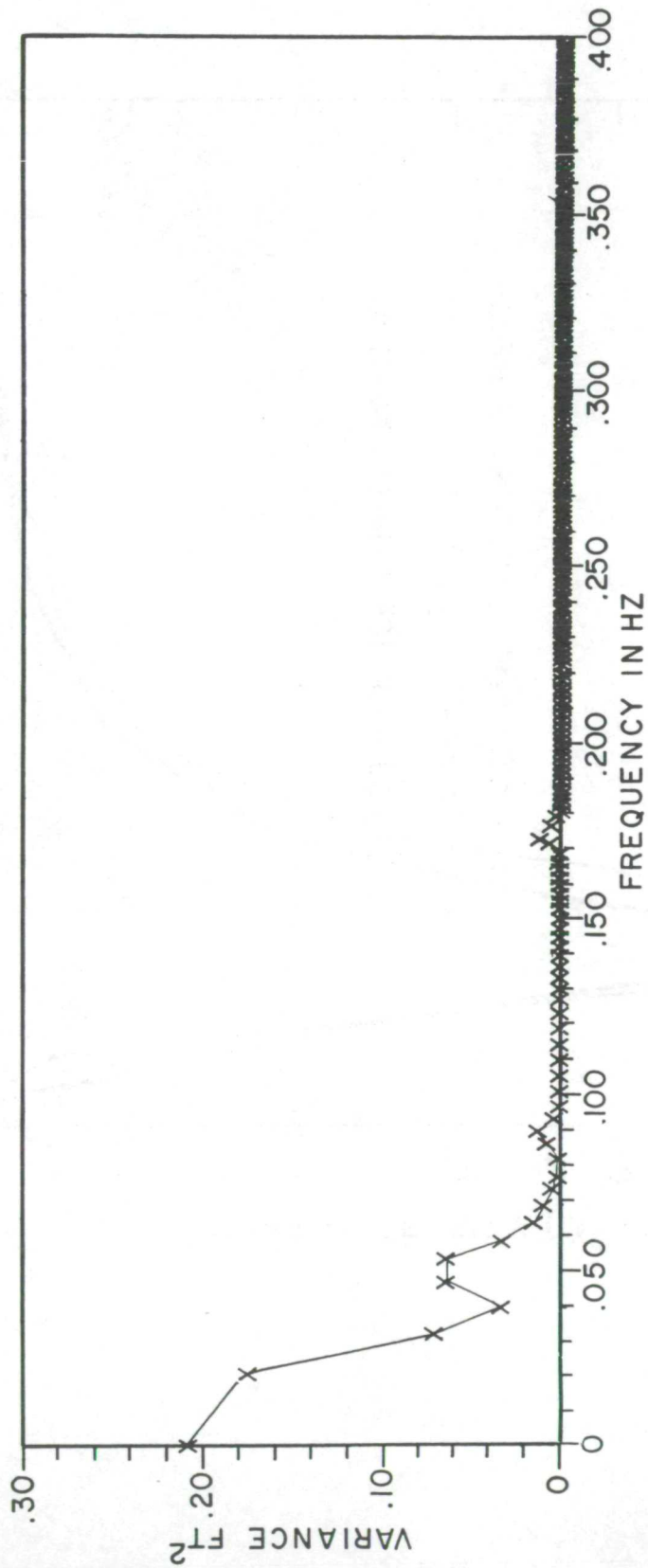


Fig. 7 Aircraft heave displacement spectrum showing energy contribution in surface wave pass band



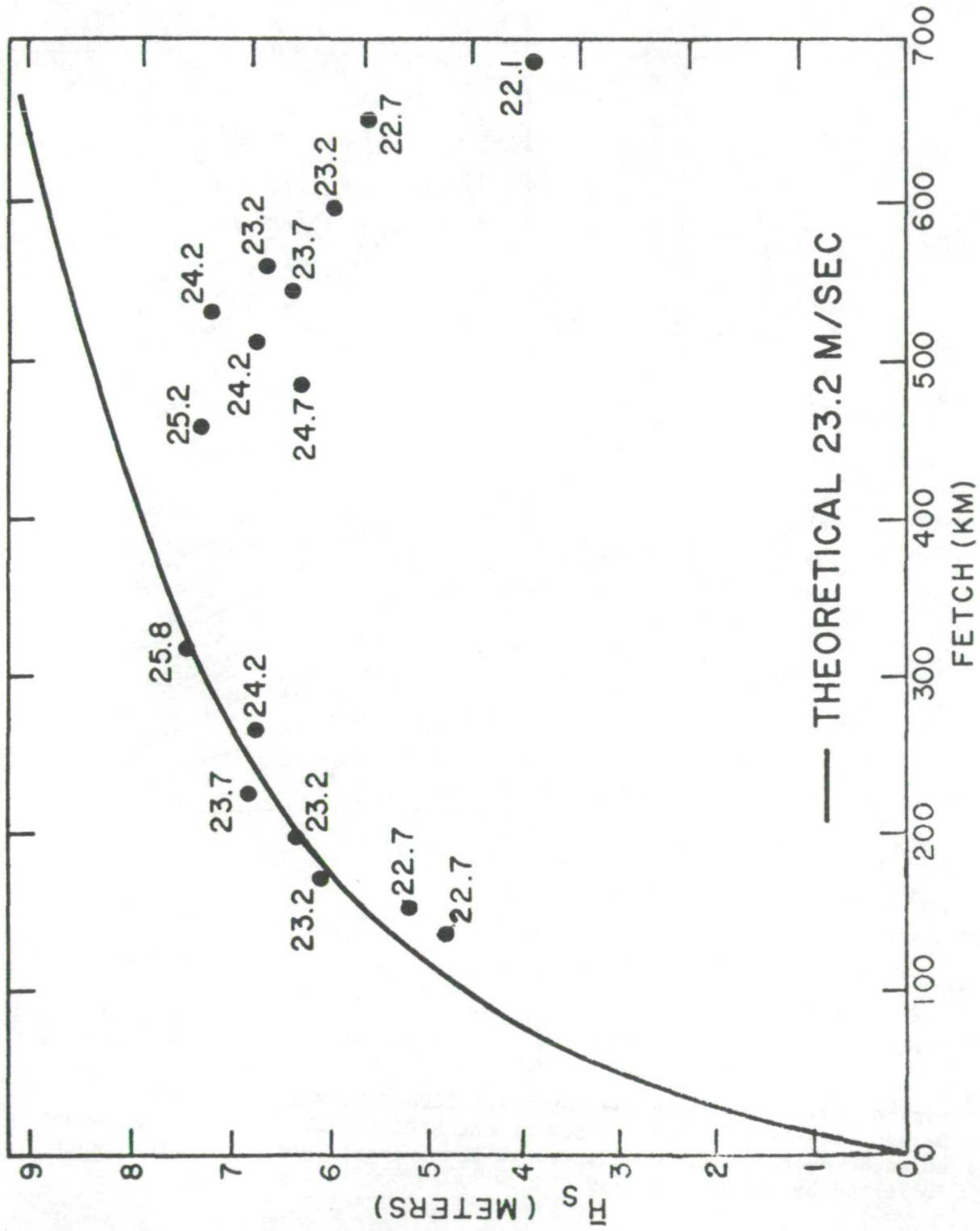
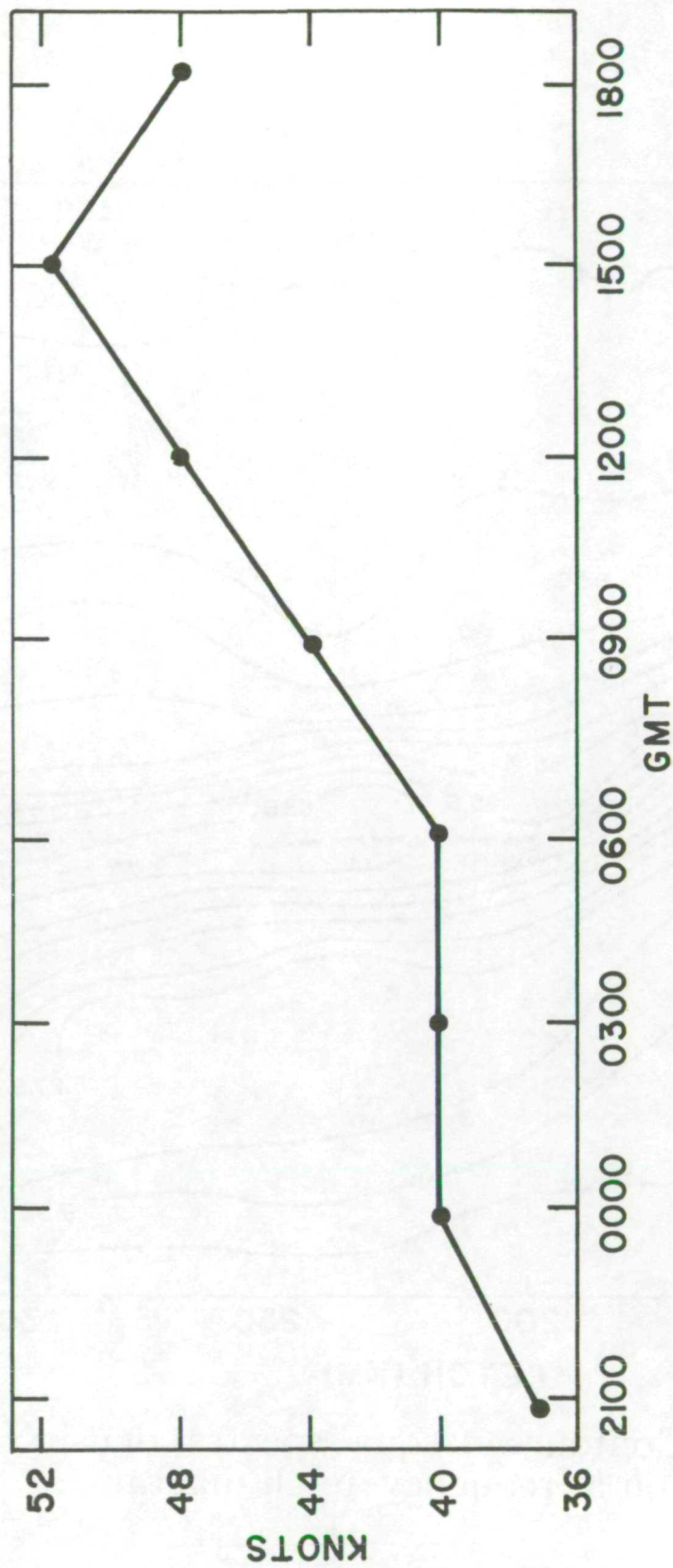


Fig. 9. Observations of significant wave height ( $\bar{H}_s$ ) as a function of fetch. Wind speeds observed in meters per second are shown next to each value.



WIND SPEEDS REPORTED BY THE GERMAN BEACON SHIP LHHT  
(57.5°N, 03°E) ON MARCH 14, 1969 AT 3 HOUR INTERVALS.

Fig. 10

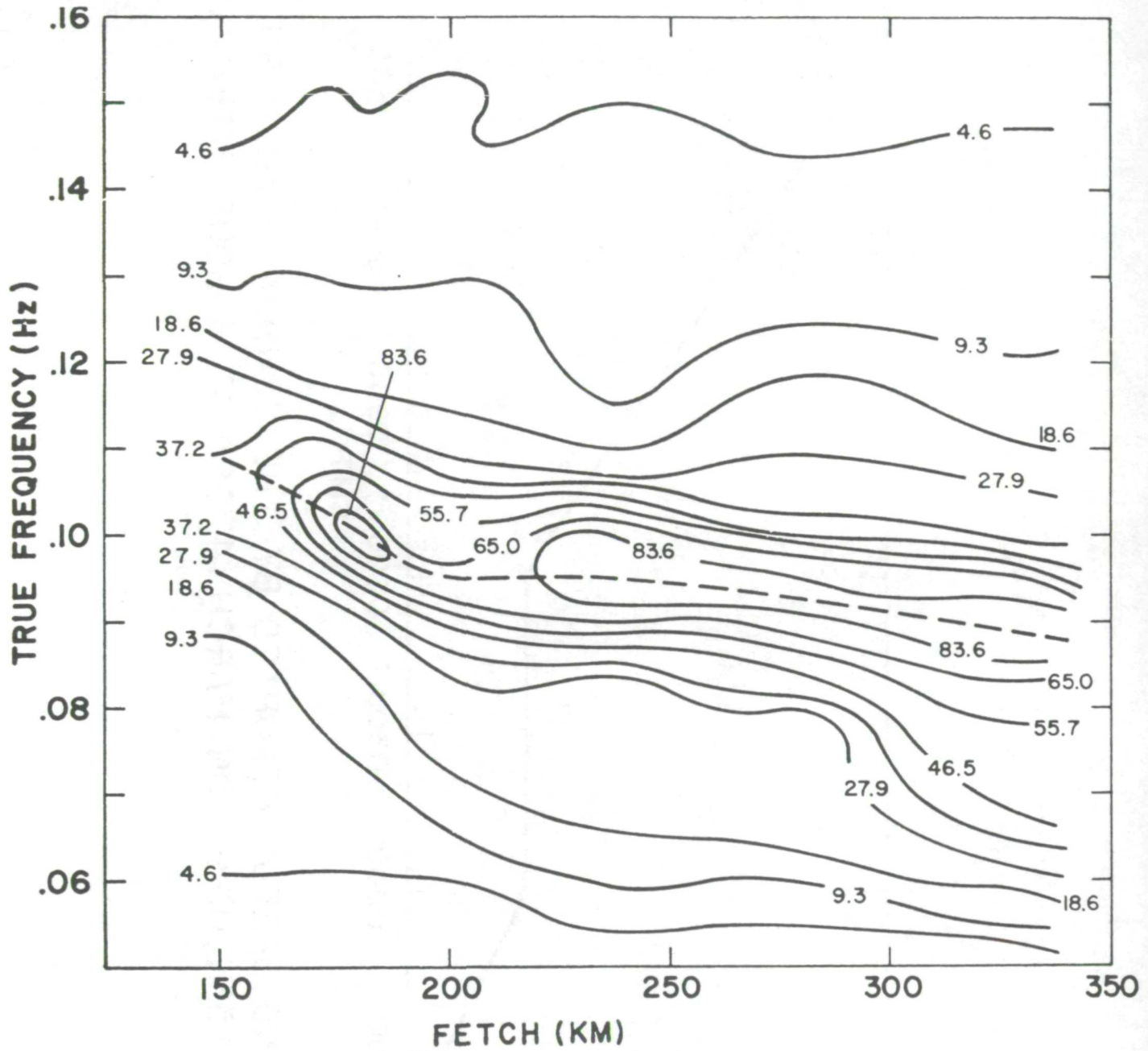


Fig. 11. Contours of equal spectral density ( $m^2 \cdot s.$ ) on a frequency-fetch diagram.

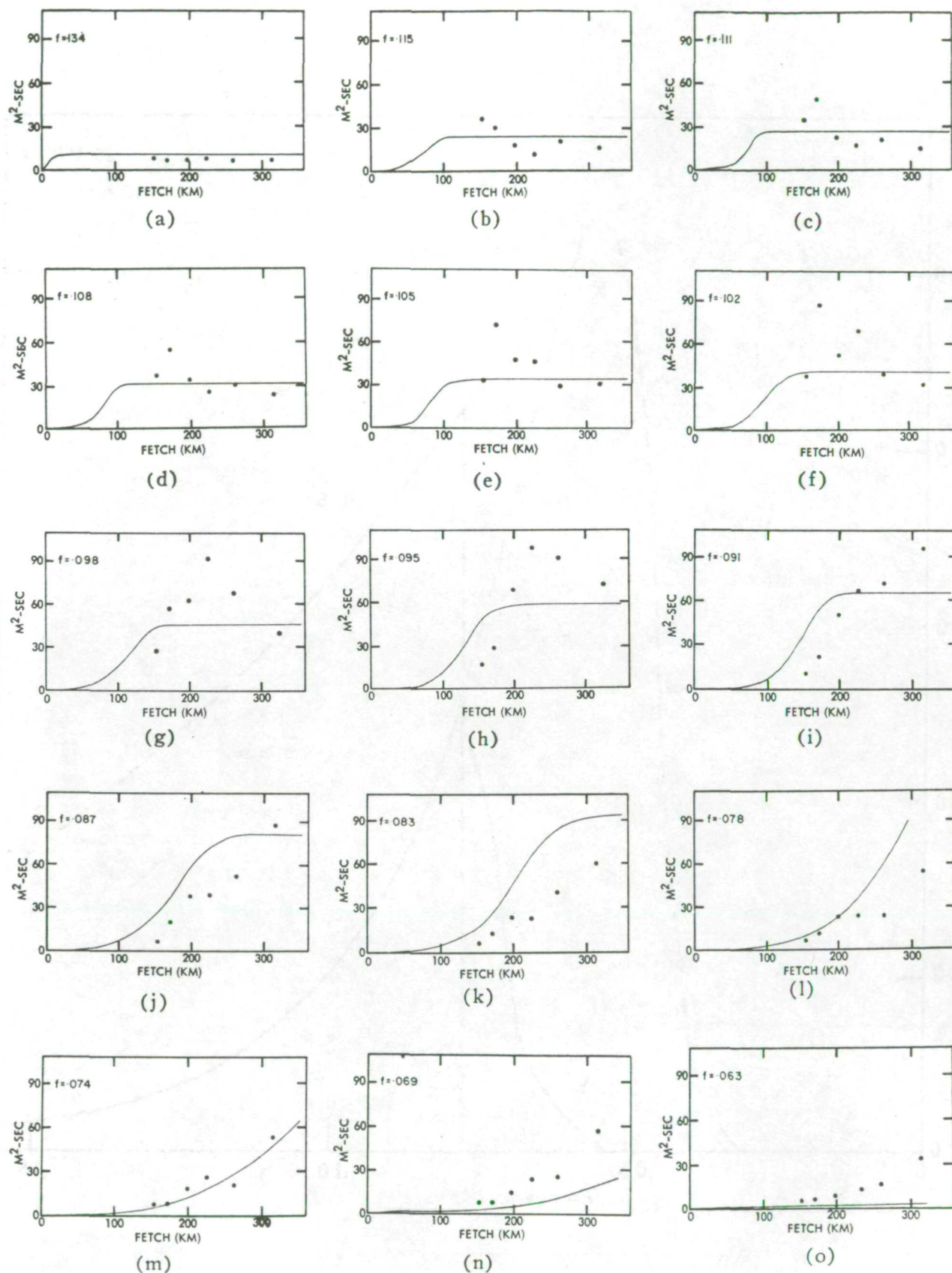


Fig. 12. Plots of spectral density versus fetch for selected frequencies.

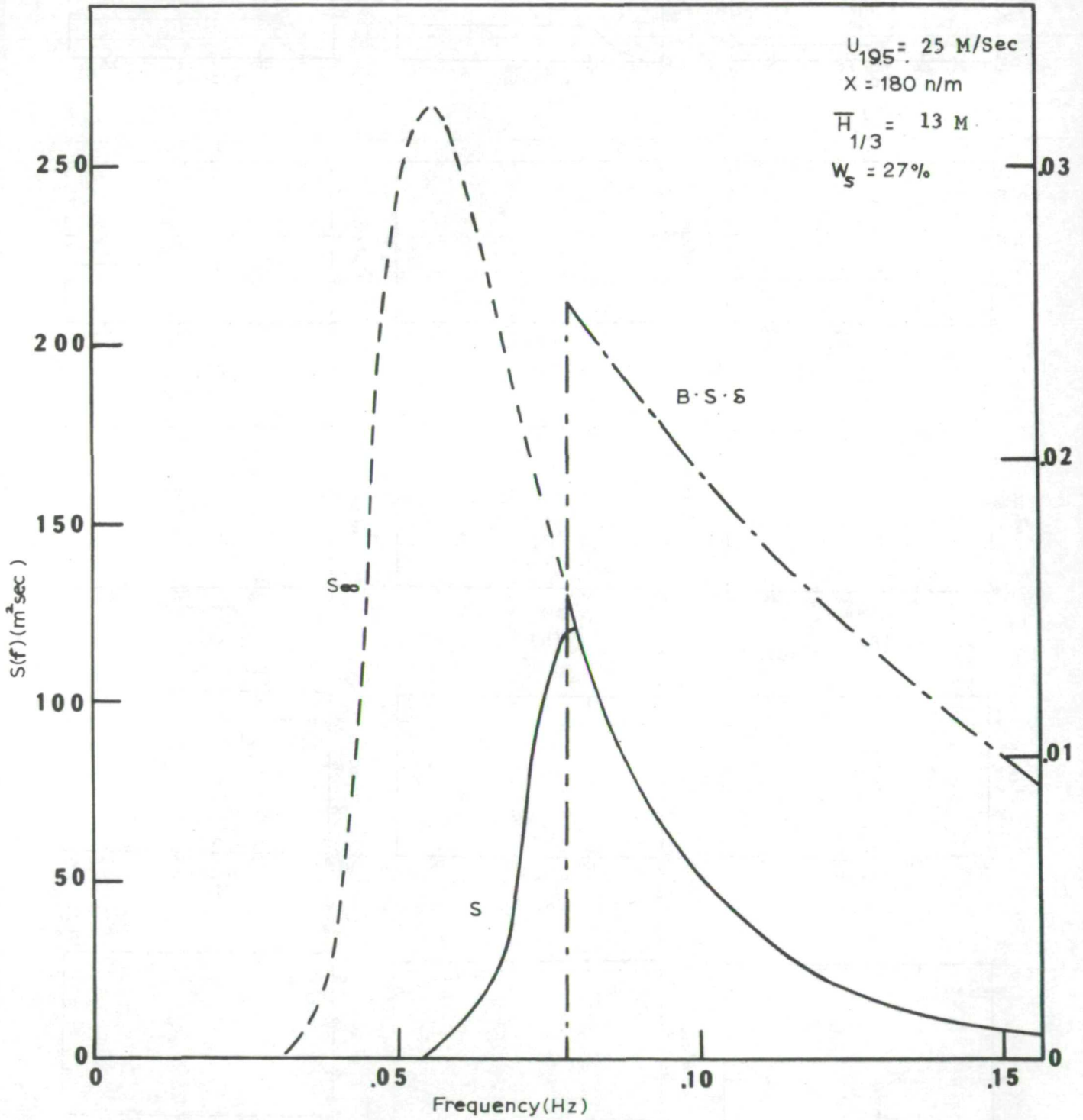


Fig. 13

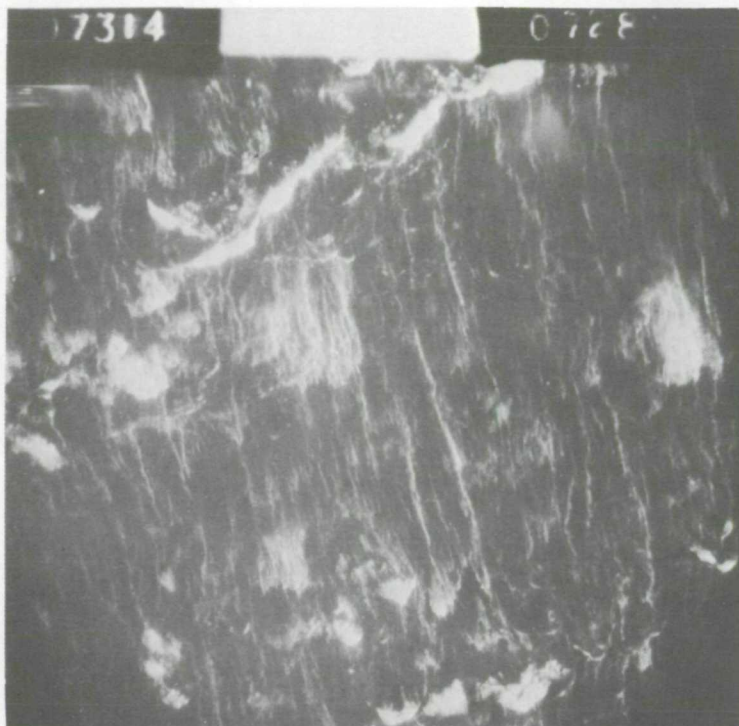


Fig. 14 25 m/sec windspeed.  
Note extensive streaking present which  
accounts for 27% of the total white water  
content of 31%.

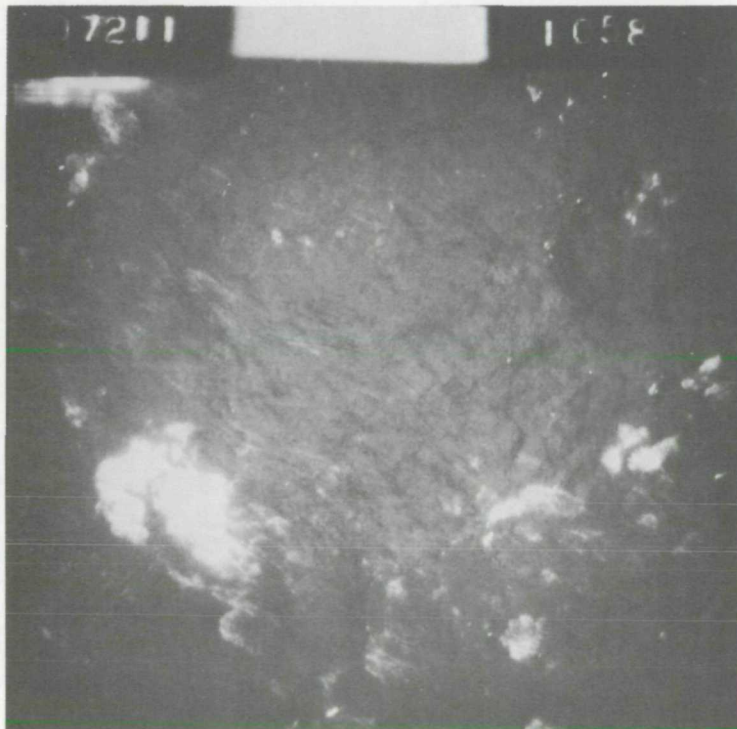


Fig. 15 12 m/sec windspeed.  
Note that thin streaks account for  
only 3% of the total of 10% white  
water.